Linear Instability of Barotropic Submesoscale Coherent Vortices Observed in the Ocean

NATHAN PALDOR

Institute of Earth Sciences, The Hebrew University of Jerusalem, Jerusalem, Israel

(Manuscript received 24 March 1997, in final form 21 July 1998)

ABSTRACT

The linear instability of circular quasigeostrophic vortices with horizontal cross sections of angular velocity identical to those that fit the observations of submesoscale eddies in the ocean is investigated analytically and numerically. The theoretical necessary conditions for instability are formulated as a single condition on the mean potential vorticity or mean angular velocity rather than the streamfunction, which is more readily applicable to oceanic lenses, eddies, and meddies. It is shown that the suggested cross sections that best fit the observed angular velocity of several long-lived vortices are all unstable to small, wavelike perturbations, and that the *e*-folding time for perturbation growth at all wavenumbers and cross sections is on the order of 1 day. For all cross sections considered, azimuthal wavenumber 1 is stable while all higher azimuthal wavenumbers, as well as all vertical wavenumbers, are unstable. The main contribution to the instability comes from the jump in potential vorticity at the radius of maximum angular velocity. When the potential vorticity is continuous at this radius, the growth rates become smaller and the details of potential vorticity distribution become important. The fast growth rates obtained by the numerical calculations clearly emphasize the insufficient spatial resolution of existing observations for deciphering the exact velocity cross sections of submesoscale oceanic vortices, especially near the radius of maximum angular velocity.

1. Introduction

Oceanic submesoscale coherent vortices (SCV) have been observed across the world's oceans since the late 1970s in the form of Mediterranean salt lenses (Schultz Tokos and Rossby 1991), Canary Basin lenses (Armi and Zenk 1984; Prater and Sanford 1994), Arctic eddies (Newton et al. 1974; Manley and Hunkins 1985), thermocline eddies in both the LDE region of Polymode (Elliott and Sanford 1986a,b; Riser et al. 1986) and the MODE region (Riser et al. 1978), and in the Beaufort Sea (D'Asaro 1988). In all these studies the azimuthal (i.e., tangential) velocity could either be calculated from hydrographic observations using the gradient wind relation or measured directly. The radial structure of the azimuthal velocity could then, in most cases, be approximated by simple expressions that best fit the observations. The linear stability of the various expressions for the azimuthal velocity suggested in the above cited observations is analyzed in this paper. In contrast to some of the observations (e.g., lenses, meddies), we ignore the vertical and azimuthal structure of the vortices and treat them as axisymmetric, barotropic (i.e., columnar) ones. Thus, the observed radial structure only motivates the stability analysis of barotropic vortices with the same radial structure as the observed ones regardless of whether or not the latter were baroclinic.

The necessary conditions for instability of a circular quasigeostrophic (QG) vortex were first derived by Fjortoft (1950). The results of linear instability theory for small, wavelike, initial perturbations, which includes in addition a semicircle theorem for the phase speed and growth rates, was subsequently summarized by Gent and McWilliams (1986), who actually calculated the instability exponents for several theoretical profiles. The application of these necessary conditions to observed profiles in atmospheric tropical cyclones or tornados was carried out by Peng and Williams (1991), but no similar application of the instability theory to oceanic vortices was attempted. The QG dynamics adopted in the latter works employs the conservation of potential vorticity and ignores density effects. These studies have all dealt with vortices characterized by a continuous potential vorticity (PV). The instability of vortices with a discontinuity (jump) in PV was investigated by Walsh (1995) and Flierl (1988). These studies used idealized PV distribution, which included a jump (e.g., piecewise uniform) but have not addressed the available observations on vortices.

A related problem to the QG instability occurs when

Corresponding author address: Dr. Nathan Paldor, Department of Atmospheric Sciences, Institute of Earth Sciences, The Hebrew University of Jerusalem, Givat Ram, Jerusalem 91904, Israel.
E-mail: paldor@vms.huji.ac.il

the vortex has a prescribed density signature, with or without an accompanying PV signature, and lies close to the surface. In this case the relative change in the isopycnal depth is not necessarily small and the quasigeostrophic approximation breaks down. Therefore, such vortices as Gulf Stream rings, which have a strong density surface signature (Olson 1991), are not included in the theory and their velocity cross sections will not be analyzed. These rings were shown (Paldor and Nof 1991) to be unstable even when the PV of the basic flow violates the QG necessary conditions for instability (e.g., when the PV is zero everywhere both within the ring and in the adjacent ocean).

As mentioned above, the purpose of this paper is to analyze several recent proposals for the azimuthal velocity cross sections (i.e., radial structure) of oceanic QG barotropic (i.e., vertically homogeneous) vortices with regard to their linear stability characteristics. In doing so I will rederive the necessary conditions for instability in section 2, casting them in terms of the angular velocity rather than the classical formulation involving the streamfunction or the potential vorticity—both of which are not directly measured in field experiments. I will then review, in section 3, the available observations of the cross sections of angular velocity of oceanic circular vortices and, for each cross section, determine whether the necessary conditions for instability are satisfied. Some of these vortices have a strong vertical structure but this baroclinic effect is ignored here and only the radial structure of these vortices will be analyzed. The application of the general necessary conditions for instability to observed barotropic vortices in the ocean as well as the derivation of some relevant analytic results are carried out in section 4. In section 5 I will present the calculations of the instabilities of observed cross sections. The findings will be discussed and summarized in section 6.

2. Circular QG vortices: Necessary conditions for instability

For completeness of presentation we briefly sketch the derivation of the governing equation. Further details can be found in Gent and McWilliams (1986). The QG conservation of PV is given by

$$Q_t + J(\Psi, Q) = 0,$$

where the subscript t denotes differentiation with respect to time and J is the horizontal Jacobian operator. The PV, Q, is related to the streamfunction, Ψ, by

$$Q = \nabla^2\Psi + f^2(\Psi_z/N^2)_z + f,$$

where f is the Coriolis parameter (assumed constant here), N is the buoyancy (Brunt–Väisälä) frequency, and the subscript z denotes differentiation with respect to the vertical coordinate. A steady solution always exists for mean, axisymmetric flows described by

$$\Psi = \overline{\Psi}(r, z), \qquad Q = \overline{Q}(r, z),$$

where r is the radial coordinate. Linear perturbations, ψ' and Q', to the mean flow satisfy

$$Q'_t + J(\overline{\Psi}, Q') + J(\psi', \overline{Q}) = 0,$$

which is the evolution equation for the perturbation PV, Q'. If we further restrict the study to barotropic (columnar) vortices, which are isolated monopoles such that $\overline{\Psi}$ (and hence $\overline{Q}$) is a function of r alone that vanishes as $r \to \infty$, then the relationship between $\overline{Q}$ and $\overline{\Psi}$ is

$$\overline{Q}(r) = (r\overline{\Psi}_r)_r/r + f.$$

We now assume that the perturbations have a normal mode form

$$\psi'(z, r, \theta, t) = \psi(r)F(z)\exp[i(l\theta - \omega t)],$$

where l and ω are the azimuthal wavenumber and frequency, $\psi(r)$ and $F(z)$ are the radial and vertical structure functions, and the latter satisfies

$$f^2(F_z/N^2)_z + m^2F = 0.$$

In a vertically bounded domain, F_z has to vanish at the boundaries to ensure that the vertical velocity vanishes there and vertically standing wave solutions exist. In an unbounded z domain, vertically propagating wave solutions exist. In the case when $N(z)$ is constant, the vertical wavenumber is given by mN/f. When the assumed normal mode form for the perturbation streamfunction is substituted for the PV in the evolution equation for Q', one obtains the following equation for the radial structure function:

$$(C - \phi)[(r\psi_r)_r/r - (l^2/r^2 + m^2)\psi] + \psi Q_r/r = 0, \quad (1)$$

where C is the phase speed (defined as $C = \omega/l$) and $Q(r)$ designates the mean PV, $\overline{Q}(r)$. The angular velocity of the basic state, $\phi(r)$, which determines the solution for ψ in Eq. (1), equals the azimuthal velocity V divided by r. The azimuthal velocity is the variable most commonly reported in field experiments and it determines the PV of the mean state, $Q(r)$, which equals $(rV)_r/r + f$. The streamfunction of the basic state does not appear in Eq. (1) but can be calculated from V by noting that $\overline{\Psi}_r = V = r\phi$. In the remainder of this section I review the analytical constraints relevant to the numerical solution of the eigenvalue problem and cast these conditions in terms of the angular velocity instead of the potential vorticity.

The eigenvalue problem, Eq. (1), for the eigenvalue C and eigenfunction ψ yields unstable modes when the phase speed $C \equiv C_r + iC_i$ has a nonvanishing imaginary part C_i (note that in the expression for C subscripts denote real and imaginary parts and not differentiation!). In order to uniquely determine the eigensolution (i.e., the eigenfunction and associated eigenvalue) this second-order equation needs two boundary conditions. The singularity of the equation at $r = 0$ requires that ψ be well behaved there and an asymptotic analysis for small values of r yields $\psi(r) \sim r^l$; $r \to 0$, which implies

$\psi(0) = 0$. The singularity at infinity implies that ψ has to vanish as r approaches infinity. An asymptotic analysis for large r shows that, when C is nonzero, $\psi(r) \sim r^{-l}$ in the vertically uniform, $m = 0$, case while $\psi(r) \sim (mr)^{-1/2} \exp(-mr)$ in the vertically varying, $m > 0$, cases.

As an eigenvalue problem Eq. (1) can be solved numerically for any value of l and m. The circular geometry, however, makes only integer values of the zonal wavenumber, l, physically acceptable, while the derivation of Eq. (1) (i.e., vanishing of the vertical velocity at the upper and lower boundaries) requires m to be an integer too. In addition, the $l = 0$ case implies zero growth rate of the perturbation, lC_i, and consequently we will restrict our discussion to integer values of $l \geq 1$ and $m \geq 0$ cases only, where $m = 0$ is the vertically uniform case relevant to barotropic perturbations and all $m > 0$ wavenumbers denote the vertically varying cases relevant to baroclinic perturbations.

To find those basic states for which Eq. (1) possesses a complex eigensolution we divide it through by $(C - \phi)$, multiply the resulting equation through by $r\psi^*$ (where ψ^* is the complex conjugate of ψ), and integrate between $r = 0$ (the axis of the vortex or any other radius where the boundary term $r\psi^*\psi_r$ vanishes) and $r = \infty$ (or some finite, large r value where the same boundary term vanishes). Since the boundary term of the integration by parts, $r\psi^*\psi_r$, vanishes at both ends $r = 0$ and $r = \infty$, the resulting equation is

$$\int |\psi|^2 \frac{Q_r(\phi - C^*)}{|\phi - C|^2} = -\int r|\psi_r|^2 \, dr - \int \left(\frac{l^2}{r^2} + m^2\right) r|\psi|^2 \, dr. \quad (2)$$

The first term on the rhs results from carrying out the integration by parts of the first term on the lhs of Eq. (1) (while making use of the vanishing of the boundary term) and C^* is the complex conjugate of C. The imaginary part of this equation is

$$C_i \int |\psi|^2 \frac{Q_r}{|\phi - C|^2} \, dr = 0, \quad (3)$$

which for $C_i \neq 0$ implies

$$\int |\psi|^2 \frac{Q_r}{|\phi - C|^2} \, dr = 0. \quad (4)$$

Thus, a necessary condition for instability is that the PV gradient of the basic flow attains both positive and negative values within the vortex. This is the analog of the ''inflection point'' necessary condition for instability of the classical barotropic QG theory in Cartesian coordinates (e.g., Drazin and Howard 1966). It should be emphasized that the necessary condition, Eq. (4), has to be satisfied only for unstable modes, whereas for stable ones—where C_i vanishes—Q_r can either vanish identically or be of one sign throughout.

The real part of Eq. (2) implies

$$\int |\psi|^2 \frac{Q_r(\phi - C_r)}{|\phi - C|^2} \, dr = -\int r|\psi_r|^2 \, dr - \int \left(\frac{l^2}{r^2} + m^2\right) r|\psi|^2 \, dr, \quad (5)$$

and for unstable modes, which satisfy Eq. (4), it is possible to replace C_r in the numerator of the integrand on the lhs of Eq. (5) by *any* constant! The natural choice is to eliminate C_r altogether (i.e., replace it by zero), which results in the necessary condition that $\phi(r)Q_r(r)$ has to be negative somewhere within the vortex for an eigenfunction to satisfy Eq. (5). Other choices of the constant to replace C_r in Eq. (5) result in equivalent necessary conditions and one such choice is $\phi(r_s)$, where r_s is the point where Q_r changes its sign (i.e., passes through zero). This is the form Gent and McWilliams (1986) used to show that if Q_r has only one zero and if, in addition, $\phi(r)$ is monotonic throughout the vortex then $[\phi(r) - \phi(r_s)]Q_r$ has to be negative *everywhere* within the vortex.

Since, in view of Eq. (4), C_r can be replaced by *any* constant, the correct form of this second necessary condition for instability should in fact read

$$(\phi(r) - \phi_m)Q_r < 0 \quad \text{for } \textit{any} \text{ constant } \phi_m, \text{ somewhere in } 0 < r < \infty, \quad (6)$$

and this modified condition includes the first, inflection point, condition as a particular case. To show this we note that, since the inequality, Eq. (6), has to hold for *any* value of ϕ_m, we can choose $\phi_m \geq \phi_{\max}$ ($\phi_m \leq \phi_{\min}$), where $\phi_{\max}$ is the maximum ($\phi_{\min}$ is the minimum) value of ϕ within the vortex and get from Eq. (6) that Q_r has to be positive (negative) somewhere within the vortex. The modified condition Eq. (6) replaces, then, the two classical conditions:

$$Q_r \quad \text{changes sign in} \quad 0 < r < \infty, \quad (7a)$$

$$\phi Q_r < 0 \quad \text{somewhere in} \quad 0 < r < \infty, \quad (7b)$$

where the latter condition obtains from Eq. (5) by using Eq. (4) to eliminate C_r on its lhs.

Using the relationship between the PV and the angular velocity, $Q = (r^2\phi)_r/r + f = 2\phi + r\phi_r + f$, these conditions can be written as

$$3\phi_r + r\phi_{rr} \quad \text{changes sign in} \quad 0 < r < \infty, \quad (8a)$$

$$3\phi\phi_r + r\phi\phi_{rr} < 0 \quad \text{somewhere in} \quad 0 < r < \infty, \quad (8b)$$

or, in a single condition analogous to Eq. (6):

$$[\phi(r) - \phi_m](3\phi_r + r\phi_{rr}) < 0 \quad \text{for } \textit{any} \text{ constant } \phi_m, \text{ somewhere in } 0 < r < \infty, \quad (9)$$

which expresses both necessary conditions for instability in a single statement.

For stable modes, where $C \equiv C_r$, an equation similar

to Eq. (5) must still be satisfied [but not Eq. (4)], which for monotonic Q throughout, that is, Q_r positive (negative) implies that C_r has to be smaller (larger) than $\phi_{\max}$ ($\phi_{\min}$).

3. Cross sections of observed oceanic SCVs

In all observations of oceanic vortices listed in the introduction the measured azimuthal velocity's cross section, $V(r)$ [which yields the angular velocity by $\phi(r) = V(r)/r$] was found to have a local extremum at some distance from the axis of the vortex. This radius of maximal azimuthal velocity, $r_{\max}$, separates the inner region located inward of the velocity maximum ($r < r_{\max}$) from the outer region where the velocity slowly decays back to zero with distance from the center of the vortex. The value of $r_{\max}$ varies considerably from close to 5 km in the Arctic and Beaufort Sea vortices (Newton et al. 1974; D'Asaro 1988) to 24 km in the Mediterranean salt lens (Schultz Tokos and Rossby 1991).

a. Inner-region cross sections

In nearly all the observations of oceanic vortices (e.g., Schultz Tokos and Rossby 1991; Prater and Sanford 1994; Newton et al. 1974; Riser et al. 1978; Armi and Zenk 1984; D'Asaro 1988) it was found that in its inner region the vortex rotates as a solid body so that the angular velocity is constant here. The rotation rate, ϕ_0, of the ''solid core'' of the vortex varies between 1.0×10^{-5} s^{-1} (Schultz Tokos and Rossby 1991) and 6.5×10^{-5} s^{-1} (Newton et al. 1974) but the existence of this solid core seems to be ubiquitous.

The only exceptions to this observed solid core radial structure in the inner region are the Mediterranean thermocline lenses observed by both Riser et al. (1986) and Elliott and Sanford (1986a,b) where the radial structure of the azimuthal velocity (at a fixed depth) in the inner region was found to best fit a Gaussian; that is,

$$V(r)/V_{\max} = (r/r_{\max})e^{[1-(r/r_{\max})^2]/2}, \qquad r \le r_{\max},$$

where $V_{\max} \equiv V(r = r_{\max})$. This Gaussian cross section is unstable when it describes the azimuthal velocity throughout the entire vortex. It is the prototype unstable profile studied intensively in Gent and McWilliams (1986) and in Peng and Williams (1991). As was shown by Gent and McWilliams (1986), this profile satisfies both necessary conditions for instability. Here, on the other hand, the Gaussian cross section describes only the inner core of the vortex so that its stability properties might be different from those of the prototype vortex described *everywhere* by a Gaussian radial structure. The validity of the observations suggesting it as a descriptor of the real cross section is questionable. In fact, this question is raised by the observers themselves; Riser et al. (1986, p. 579) emphasize that: ''It should be noted that this model (i.e., the Gaussian best fit) is not a unique descriptor of the eddy structure and can probably not be distinguished statistically from other simpler models.'' The Gaussian profile in the inner region shown in Fig. 18 of Elliott and Sanford (1986a) is based on observations of azimuthal velocity, which are all too clustered near $r_{\max}$ to yield a fit significantly different (statistically) from a straight line. Lack of sufficient observations closer to the center of the vortex is also manifested in the high velocities used for the comparison in Fig. 5 of Elliott and Sanford (1986b) where no data is available at azimuthal velocities lower than half the maximal velocity observed in the vortex. The calculated geopotential anomaly cross sections shown in Fig. 4 of Elliott and Sanford (1986b) contain only three points at $r < r_{\max}$ (where $r_{\max}$ is determined by the radius of maximum gradient of the geopotential anomaly) and it, too, can hardly be confidently distinguished from a parabolic one commensurate with a linear azimuthal velocity cross section.

Thus, we conclude that, except for two fairly questionable findings of a Gaussian inner region, the inner region of nearly all observed oceanic QG vortices is characterized by a stable solid body rotation at uniform angular frequency slightly below the Coriolis frequency. The solid body rotation results in vanishing mean PV gradients, $Q_r = 0$, which is, in itself, stable as it does not satisfy the necessary condition for instability. The PV gradient of a Gaussian angular velocity is $Q_r = e^{(1 - r^2)/2}(r^2 - 4)r$, where $r = 1$ defines the perimeter of the inner region (see below).

b. Outer region profiles

The ubiquitous existence of a radius of velocity maximum $r_{\max}$ suggests that it be used as the length scale for all radial distances. If we further take the azimuthal velocity at this distance, $V_{\max}$, to be the velocity scale, then the scaled angular velocity, $\phi(r) \equiv V(r)/r$, too equals 1 at the radius $r = 1$ separating the inner and outer regions. It is clear, therefore, that the continuity of $V(r)$ at $r = 1$ ensures that of $\phi(r)$ there and from this point on, we will refer to the scaled variables only. Observed cross sections of azimuthal velocity, $V(r)$, outside the velocity maximum (i.e., for $r > 1$) were all found in various oceanographic expeditions to have a noncompact PV distribution and the best fit to the observations are given by one of three possible expressions.

Exponential: $V(r) = e^{a(1-r)}$
(Schultz Tokos and Rossby 1991; Elliott and Sanford 1986a);
Gaussian: $V(r) = e^{a(1-r^2)}$
(D'Asaro 1988; Riser et al. 1986);
Algebraic: $V(r) = r^{-a}$
[Prater and Sanford (1994), Newton et al. (1974), and a second suggestion by Schultz Tokos and Rossby (1991)].

Note that the Gaussian outer-region cross section differs from the inner-region one by the r factor required in the latter to ensure that the azimuthal velocity vanishes at $r = 0$ (i.e., that the angular velocity is finite there). It should also be noted that although the form of decay is limited to three expressions only, the numerical value of a in all these expressions, which determines the rate of decay of the velocity at infinity, varied significantly between observations. In two field observations of SCV—the one described in Armi and Zenk (1984) and that described in Riser et al. (1978)—no attempt was made to infer the radial structure of azimuthal velocity from the hydrographic measurements.

From the expressions given above for the azimuthal velocity, $V(r)$, one can calculate the angular velocity, $\phi(r) \equiv V(r)/r$; the PV, $Q \equiv 2\phi + r\phi_r$; and the PV gradient, $Q_r \equiv 3\phi_r + r\phi_{rr}$. The latter two, which determine the stability of each of these radial SCV structures, are given by

1) Exponential: $Q = e^{a(1-r)}(1/r - a)$,
$$Q_r = e^{a(1-r)}(a^2 - a/r - r^{-2}).$$
This PV gradient changes sign only for $ar < (1 + \sqrt{5})/2$ and has a root at some $r > 1$ only if $0 < a < 1.62$.
2) Gaussian: $Q = e^{a(1-r^2)}(2ar - 1/r)$,
$$Q_r = e^{a(1-r^2)}(4a^2r^2 - 4a - r^{-2}).$$
This PV gradient changes sign only for $a \cdot r^2 < (1 + \sqrt{2})/2$ and has a root at some $r > 1$ only if $0 < a < 1.21$.
3) Algebraic: $Q = r^{-(a+1)}(1 - a)$,
$$Q_r = r^{-(a+2)}(a^2 - 1).$$
This PV gradient is positive for $a > 1$ and negative for $a < 1$ but it never (i.e., not even for $a = 1$) changes sign! Therefore, we expect this cross section to be stable regardless of the value of a. The instability of these three types of outer cross sections is investigated in the next section.

4. Analytical results and jump condition for observed SCVs

Observed SCVs in the ocean are all interpreted as having a discontinuous radial derivative of the angular velocity (but the angular velocity itself, as well as, the radial and azimuthal velocities are, of course, all continuous). Therefore, the necessary conditions derived in section 2 for a general QG vortex and not accounting for the possibility of a discontinuity have to be applied to the relevant case of observed SCVs, where ϕ_r, and hence Q_r, both have a jump at the boundary of the inner region, $r = 1$. The accepted cross section in the inner region of observed SCV is that of a solid body rotation, that is, constant angular velocity. The suggestion of a Gaussian angular velocity in the inner region is fairly rare and uncertain, which makes it reasonable to try to solve the problem in the case of a solid body inner region as a starting point for a general numerical solution of the eigenvalue problem. The structure of the analytic solution in the inner region can then serve as a check on the numerically computed eigenfunctions. Both points are handled in this section as a prelude to the numerical solution of the eigenvalue problem in section 5.

a. The eigenfunction in the solid body inner region

When the inner region rotates as a solid body with $\phi(r) = 1$ and $Q_r = 0$ at $0 \le r \le 1$, the eigenvalue equation (1) has a trivial, stable, solution with $C = \phi = 1$. For eigensolutions with $C \neq \phi$ (which includes the unstable case) the eigenvalue C drops out of the equation while the eigenfunction $\psi(r)$ in that interval obtains as a solution of the equation:

$$(r\psi_r)_r - (l^2/r + rm^2)\psi = 0. \tag{10}$$

The solution for $\psi(r)$ is given by $J_l(imr)$, where J_l is the Bessel function of the first kind of order l. Instead of evaluating the values of Bessel functions for imaginary arguments, a series expansion sheds more light on the behavior of the solution. The nature of the singularity of this equation at $r = 0$ (a removable singularity) implies that for a general (l, m) pair the regular solution near $r = 0$ can be expanded in a Frobenius series in powers of r;

$$\psi(r) = \sum_{n=0}^{\infty} a_n r^{\alpha+n}, \qquad a_0 \neq 0.$$

When this expansion is substituted in Eq. (10), one finds that $\alpha = l$ and that the recursion relation for the coefficients, $\{a_n\}$, is

$$\frac{a_n}{a_{n-2}} = \frac{m^2}{n(l + n)}, \qquad n \ge 2.$$

Therefore, in the case $m = 0$ all the coefficients of the infinite series with index $n > 0$ vanish so that the *exact* solution throughout the entire range $0 \le r \le 1$ reduces to $\psi(r) = r^l$ in this case. For $m \neq 0$ the Frobenius series contains even powers of r only [this is due to the symmetry of Eq. (10) with respect to the r] and its convergence at $r = 1$ is fast (quadratic in n for fixed m). This simple solution is independent of C and can be used in two ways when solving the eigenvalue problem, Eq. (1). The first way is to integrate Eq. (1) numerically in the outer region only and impose the value of the logarithmic derivative of the analytic solution in the inner region (e.g., $\psi'/\psi = l$ for $m = 0$) as a boundary condition on the solution in the outer region at $r = 1$. The second way to use this analytic solution is to integrate Eq. (1) numerically in *both* regions and validate the results of the numerical integration by comparing the inner-region numerical solution with the analytic one. In the present study the analytic solution was employed to provide an independent check on the validity of the numerical results.

b. The jump condition

When Q_r is discontinuous (i.e., has a jump), as it is at $r = 1$ in the case of all observed SCVs, any integration from $r = 0$ to $r = \infty$ similar to those derived in section 2 should be carried out explicitly in three different intervals: The first interval is $(0, 1 - \epsilon)$; the second is $(1 - \epsilon, 1 + \epsilon)$; and the third is $(1 + \epsilon, \infty)$, where ϵ is some infinitely small number. The middle interval represents the contribution due to the discontinuity in PV at $r = 1$. In the case of a solid body rotation in the inner region, Q_r vanishes identically there, so there is no contribution to the integrals in Eqs. (3) and (5) from the $r \leq 1$ range. Thus, if the contribution to these integrals due to the jump in PV at $r = 1$ is ignored, the necessary conditions for instability, Eqs. (7) or (8) have to hold in $r > 1$, which, as was shown in section 3, limits the range of a values where instabilities can exist.

One way of taking the jump in Q_r at $r = 1$ into account is to carry out a direct integration of Eq. (1) in the middle range, $(1 - \epsilon, 1 + \epsilon)$, taking into account the continuity of $\phi(r)$ at $r = 1$. The continuity of *radial* velocity there implies that $\psi(r)$, too, has to be continuous at $r = 1$. Carrying out the integration and then taking the limit $\epsilon \to 0$ results in the jump condition on $\psi_r(1)$:

$$\psi_r(1^+) - \psi_r(1^-) + \frac{\psi(1)}{C - \phi(1)}(Q(1^+) - Q(1^-)) = 0. \tag{11}$$

For a continuous PV at $r = 1$ the PV jump satisfies $Q(1^+) - Q(1^-) = 0$ and the matching condition implies the continuity of $\psi_r(r)$ at $r = 1$. For all observed SCVs, however, $Q(r)$ itself [i.e., not only $Q_r(r)$] has a jump at $r = 1$, which requires $\psi_r(r)$ to be discontinuous there too. The solution of the eigenvalue problem using this jump condition at $r = 1$ for observed SCVs is described next.

5. Numerical calculation of the instabilities

The solution of the eigenvalue problem involves integrating Eq. (1) numerically in the inner region (using the asymptotic solution near $r = 0$ as an initial condition) and in the outer region (starting from the asymptotic solution at infinity) and then matching the two solutions at $r = 1$ using the jump condition Eq. (11). This procedure involves either integrating the equation in the outer region over a very large radial interval or imposing the asymptotic expansion at $r = \infty$ at $O(1)$ values of r. In order to overcome this difficulty and employ the matching of the solutions efficiently, a transformation of the radial variable to a variable that covers a finite range as r varies between 0 and ∞ has been used. Both the transformation of variables and the application of shooting method to the transformed variable are described in this section.

a. Transformation of variables

In order to overcome the difficulty of integrating over infinitely large intervals of r, the transformed independent variable: $x \equiv r/(1 + r)$ is defined. In terms of this transformed variable the origin, $r = 0$, transforms to $x = 0$ while $r = \infty$ transforms to $x = 1$. The radius of maximal velocity, $r = 1$, where the jump condition has to be applied transforms to $x = 1/2$. Radial derivatives transform according to

$$\frac{\partial}{\partial r} = (1 - x)^2 \frac{\partial}{\partial x}.$$

The transformed variable x is used for integrating Eq. (1) in the inner region, $0 \leq x \leq 1/2$, starting from the asymptotic solution $\psi(x) \sim x^l$ near $x = 0$ while $X \equiv 1 - x = 1/(1 + r)$ is used for integrating Eq. (1) in the outer region [$r > 1$ starting from the asymptotic solution (which is different for $m = 0$ and $m > 0$)] at $r = \infty$, that is, $X = 0$. The transformation of X derivatives to r derivatives is according to

$$\frac{\partial}{\partial r} = -X^2 \frac{\partial}{\partial X}.$$

b. The shooting method

The shooting method employed in the present study is similar to the one employed successfully in several other singular eigenvalue problems described, for example, in Paldor and Ghil (1990) and Paldor and Nof (1991). In the present application of this shooting method the transformed version of Eq. (1) is integrated numerically using a double precision, fourth-order Runge–Kutta scheme with a 10^{-8} tolerance. Two such integrations were carried out: the first one, in the inner region, was carried out between $x = 10^{-5}$ starting with $\psi(x) = x^l$ (thus making sure that the boundary condition at the origin is satisfied) and the matching point $x = 1/2$ and the values of both $\psi(\frac{1}{2}^-)$ and $\psi_x(\frac{1}{2}^-)$ were stored. The second integration was carried out from near $X = 0$ (see the precise values below) to $X = 1/2$ starting with either $\psi(X) = X^l$ for $m = 0$ or $\psi(X) = (X/m)^{1/2} \exp(-m/X)$ for $m > 0$ and the resulting values of ψ and ψ_r at the matching point $X = 1/2 = x$, $\psi(\frac{1}{2}^+)$ and $\psi_X(\frac{1}{2}^+)$ were stored. Due to the vastly different rate of decrease of $\psi(X)$ near $X = 0$ for the two cases $m = 0$ and $m > 0$ the integration was originated at $X = 10^{-5}$ (which corresponds to $r = 10^5$) for the $m = 0$ cases and $X = 0.05$ ($r = 20$) for the $m > 0$ cases since at smaller values of X the initial value of $\psi(X)$ could not be numerically distinguished from 0. The derivatives with respect to x and X were then transformed back into r derivatives.

In order to apply the jump condition, Eq. (11), the calculated eigenfunction in the outer region and its radial derivative were both divided through by $\psi(\frac{1}{2}^-)$ (which never vanishes according to the analytical solution found in the preceding section), which ensures

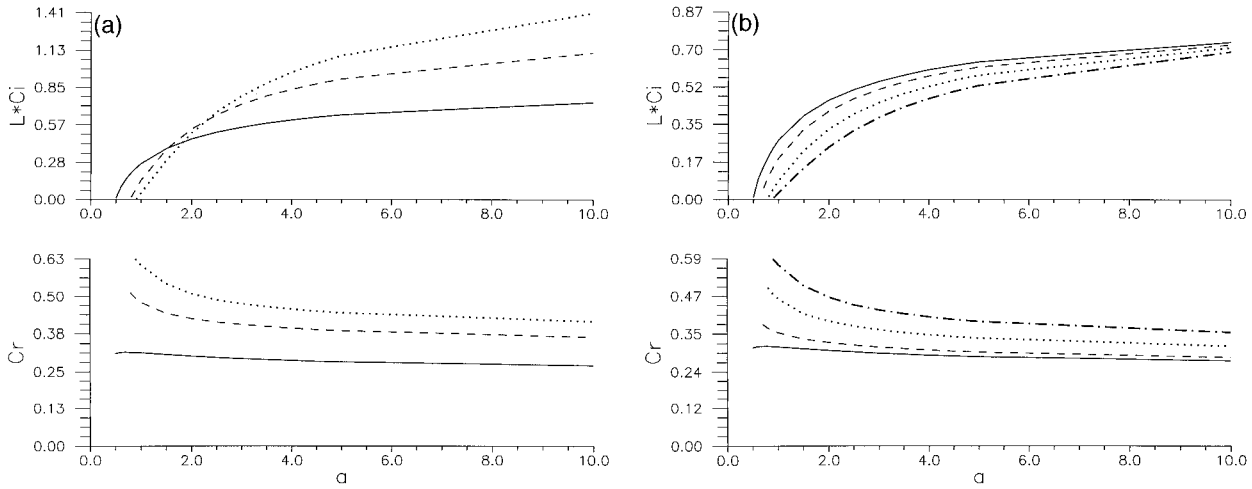

FIG. 1. The eigenvalues for the solid body inner region; Gaussian outer-region cross sections as a function of outer region decay rate a. (top) The growth rate lC_i; (bottom) the phase speed C_r. The results for barotropic perturbations ($m = 0$) are given in (a) for $l = 2$ (solid curve), $l = 3$ (dashed curve), and $l = 4$ (dotted curve) and those for azimuthal wavenumber 2 (both baroclinic and barotropic perturbations) are given in (b) for $m = 0$ [solid curve, same as in (A)], $m = 1$ (dashed curve), $m = 2$ (dotted curve), and $m = 3$ (dashed-dotted curve).

the continuity of $\psi(r)$ at $r = 1$. The jump condition on the resulting radial derivatives [i.e., after the derivative of the outer region solution at the matching point, $\psi_r(1^+) = -\frac{1}{4}\psi_x(\frac{1}{2}^+)$, is divided through by $\psi(\frac{1}{2}^-)$ and $\psi_r(1^-) = \frac{1}{4}\psi_x(\frac{1}{2}^-)$ is used for the radial derivative of inner region solution at $r = 1$] is precisely Eq. (11). The value of C is then varied until the jump condition, Eq. (11), is satisfied.

c. Growth rates for the solid body inner-region cross section

In the following we calculate the PV jump at $r = 1$ for the three outer-region cross sections described in section 3 for the case of a solid body rotation in the inner region and calculate the resulting growth rates obtained when the eigenvalue equation is solved. The PV in the inner region equals 2 so that $Q(1^-) = 2$ when the angular velocity equals 1 there while its value in the outer region varies according the assumed profile of angular velocity there. The PV jump at $r = 1$ varies, therefore, from one profile to another.

1) GAUSSIAN OUTER CROSS SECTIONS

From the expression given at the end of section 3, $Q(1^+) = (1 - 2a)$ so that the PV jump at $r = 1$ satisfies $Q(1^+) - Q(1^-) = (-1 - 2a)$. The resulting phase speeds for the unstable cases are shown in Fig. 1a for barotropic perturbations ($m = 0$) and $l = 2, 3, 4$ and in Fig. 1b for azimuthal wavenumber 2 and $m = 0, 1, 2, 3$, that is, both barotropic and baroclinic perturbations. No growing modes were found for $l = 1$.

2) EXPONENTIAL OUTER CROSS SECTION

Here, $Q(1^+) = (1 - a)$ so that the PV jump at $r = 1$ equals $(-1 - a)$. The resulting complex phase speeds for barotropic ($m = 0$) perturbations are given in Fig. 2a for $l = 2, 3, 4$. In Fig. 2b the resulting complex phase speeds for azimuthal wavenumber 2 are given for $m = 0, 1, 2, 3$ (i.e., barotropic and baroclinic perturbations). Azimuthal wavenumber 1 is stable.

3) ALGEBRAICALLY DECAYING OUTER CROSS SECTIONS

The value of $Q(1^+)$ for this cross section is $(1 - a)$ the same as for the exponential cross section so that the PV jump at $r = 1$ equals $(-1 - a)$ and the results for the growth rates of this profile are shown in Fig. 3 for the same values of m and l as in other two outer-region cross sections. In this case, too, $l = 1$ is stable.

d. Gaussian inner-region cross sections

When the angular velocity in the inner region is assumed to vary as $\phi(r) = e^{(1-r^2)/2}$, the PV at the matching point, $Q(1^-)$, equals 1, while the PV gradient in the inner region is given by $Q_r(r) = e^{(1-r^2)/2}(r^2 - 4)r$. In the case of a Gaussian outer-region cross section [recall that the Gaussian cross sections are not identical in the two regions: the inner region angular velocity does not contain the $(1/r)$ factor, which multiplies the $e^{a(1-r^2)}$ in the outer region] the PV jump at $r = 1$ equals $(-2a)$. The resulting complex phase speeds that solve the eigenvalue problem are shown in Fig. 4. Similar results were obtained for the other outer cross sections (not shown).

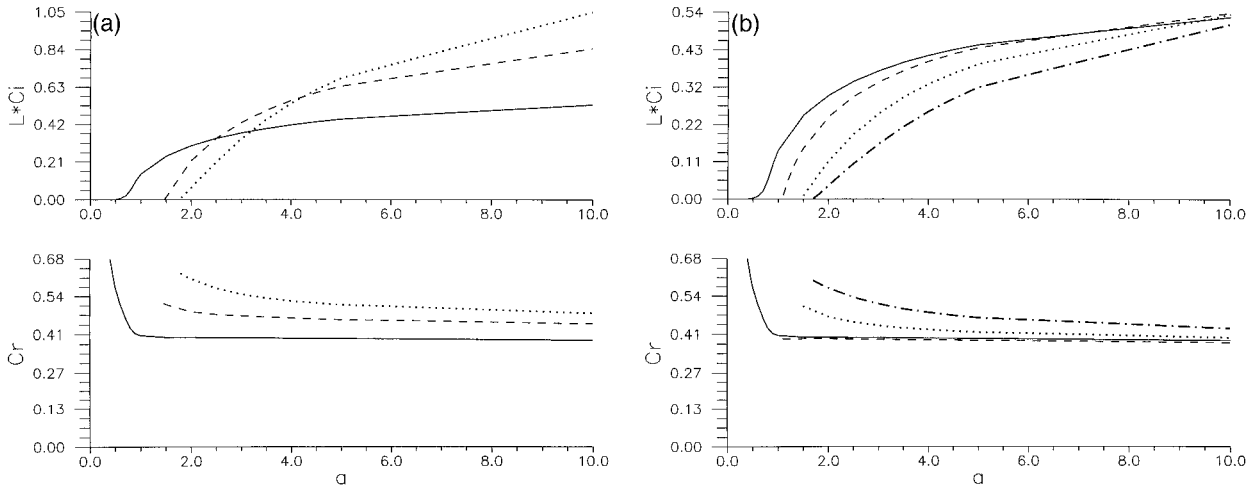

FIG. 2. Same as in Fig. 1 but for an exponential outer-region cross section.

6. Discussion and summary

The present study focuses on the instability of barotropic axisymmetric (columnar) vortices with the same radial structure as that observed in oceanic SCVs when the mean state is independent of the vertical coordinate, *z*. All available observations were interpreted so as to yield a discontinuous radial derivative of the angular momentum, which results in a discontinuous PV at the edge of the inner region. The results of the calculations shown in Figs. 1–4 clearly demonstrate that observed SCVs in the ocean are all highly unstable and that the growth rate of the unstable modes is nearly independent of the details of cross section assumed for the angular velocity in the vortex. This instability owes its existence to the discontinuity in PV. In cases where the angular velocity cross section yields a continuous PV this instability disappears and, unless the necessary condition for instability [e.g., Eq. (7)] is satisfied by the PV, the vortex is stable. The prime example for this is the SCV with algebraically decaying outer-region cross section: According to the analysis presented in section 3, this vortex is stable in the continuous case but the results shown in Fig. 3 clearly indicate that it is highly unstable when the PV is discontinuous. The same holds true for large values of a at which the exponential and Gaussian outer-region cross sections are stable, according to the analysis in section 3, when the PV is continuous but were found to be unstable (see Figs. 1 and 2) when Q has a jump. Even a change of the inner-region profile from a solid body rotation to Gaussian angular velocity does not have a significant effect on the growth rates (e.g., Fig. 4). This combination of Gaussian inner- and outer-region cross sections does not impose any restriction on the value of a where instabilities can be found as the PV gradient for $r < 1$ is always negative while for $r \gg 1$ it is always positive. (Similar calculations of

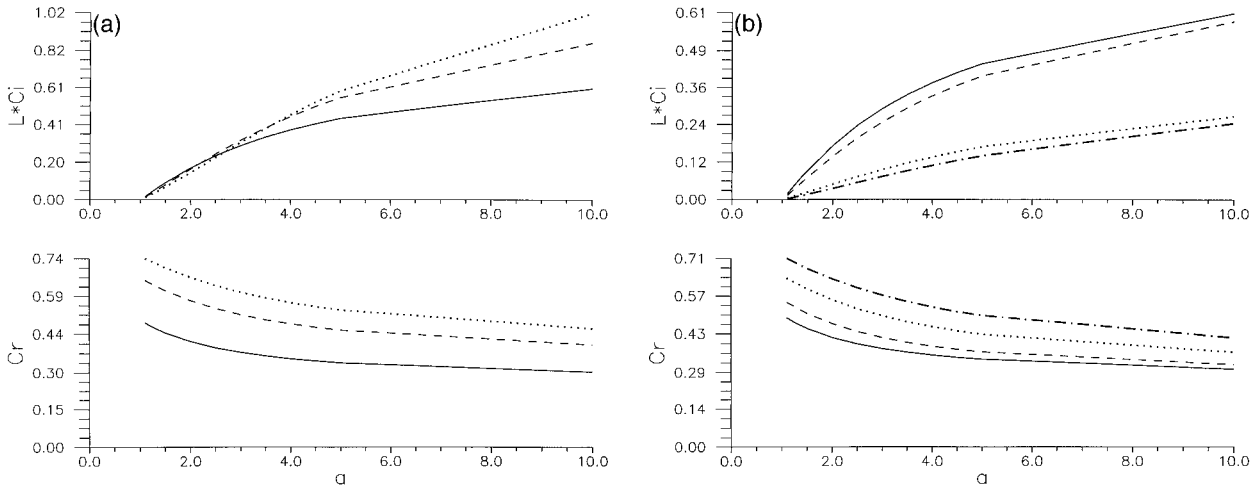

FIG. 3. Same as in Fig. 1 but for an algebraically decaying outer-region cross section.

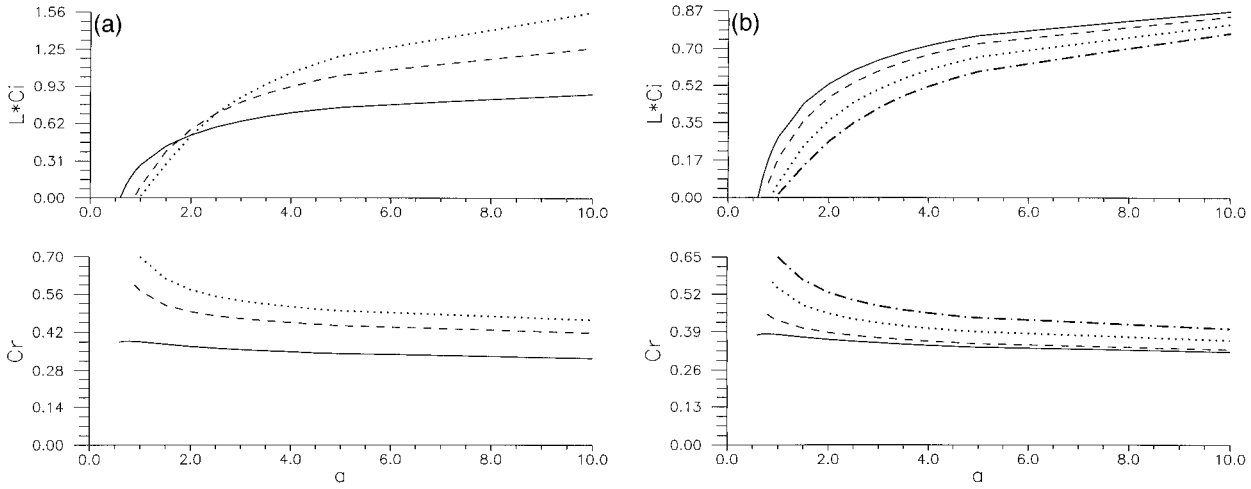

FIG. 4. The effect of nonuniform angular velocity in the inner region. The outer-region cross section is Gaussian; in the inner region the angular velocity is given by $\phi(r) = e^{(1-r^2)/2}$. The results are displayed as in Fig. 1.

the growth rates made at selected values of a with exponential and algebraic outer-region cross sections for the Gaussian inner-region cross section have resulted in growth rates very similar to those with a solid body rotation in the inner region). The existence of finite growth rates at large values of a regardless of the cross section assumed in the outer region makes it plausible that an asymptotic theory might exist, which provides an estimate of C_i in the limit $a \to \infty$. This is left for future work.

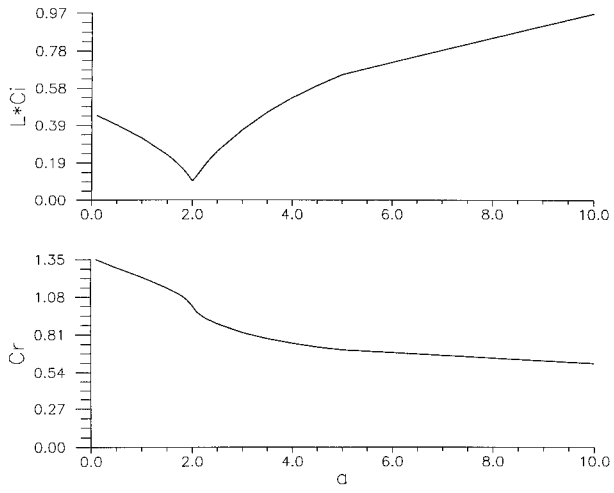

FIG. 5. The change in growth rate when the PV jump at $r = 1$ vanishes. The inner-region cross section is a concocted one (see text for details), which yields a continuous PV at $r = 1$ in the case of an algebraically decaying outer-region cross section at $a = 2$. The PV gradient, Q_r, is negative in the inner region; in the outer region it is positive for $a > 1$ and negative for $a < 1$. Thus, the instability for $a < 1$ is due entirely to the jump in PV while that at $a = 2$ is due entirely to the inflection point, change is sign of Q_r instability. In the ranges $a > 2$ and $1 < a < 2$ the instability is mixed and it is evident from this figure that the instability in these ranges of a is dominated by the PV jump.

To illustrate the role of the discontinuity of ϕ_r (and Q) at $r = 1$, an inner-region cross section of angular velocity was concocted that has a negative Q_r in this region. This inner-region cross section was augmented with an algebraically decaying outer-region profile. For $a > 1$, Q_r is positive in the outer region according to section 4 so that the combined cross section satisfies the necessary conditions for instability derived in section 3 since Q_r changes sign between the inner and outer regions. When the two cross sections result in a continuous PV, the instability is the typical ''inflection point'' one, while when the PV has a jump the instability encountered in Figs. 1–4 is realized. The specific inner-region cross section employed for this comparison is $\phi(r) = [1 + b(1 - r)(2 - r)]e^{(1-r^2)/2}$, which yields a monotonically decreasing PV in that region ($Q_r < 0$) for all $b > 0$. The values of angular velocity and PV at $r = 1$ are $\phi(1^-) = 1$ and $Q(1^-) = (1 - b)$ so that from the calculation given in section 5c(3) ϕ is continuous at $r = 1$ for all values of a and b while the PV jump there equals $(b - a)$. For $b = 2$ we get the $C_i(a)$, $C_r(a)$ curves shown in Fig. 5 ($l = 2$, $m = 1$), which clearly demonstrates that the instability remains large only as long as the PV has a jump at $r = 1$ and it decreases significantly at $a = 2 = b$ where the PV jump vanishes. The instability at this value of a is due only to the inflection in PV, and this dip in C_i is accompanied by an abrupt change in C_r. In the range $a < 1$, Q_r in the outer region becomes negative so that the inflection point necessary condition for instability is not satisfied and the instability is due entirely to the jump in PV.

An interesting result that appears in all cross sections is the stability of azimuthal wavenumber 1. This numerical finding can be shown analytically (G. R. Flierl

1998, personal communication) to hold for barotropic perturbations, $m = 0$, regardless of the assumed cross section. In baroclinic cases ($m > 0$) instabilities were indeed found at $l = 1$ in both Gent and McWilliams (1986) and Flierl (1988).

As it is, the theory cannot be applied straightforwardly to lenses or meddies that have strong vertical dependence but can only serve as a check on their suggested radial structure. The inclusion of vertical variation of the mean PV renders the basic state too complex to analyze by the simple methods described here. We anticipate that a vertical dependence of the mean state will have a destabilizing effect on the vortex since baroclinic instability is filtered out of the present theory. A demonstration of a destabilizing baroclinic effect in circular vortices is provided by Walsh (1995) where a linear variation of Q with z in a vortex with algebraic radial structure turns the vortex unstable only for large enough Q_z.

Fractional wavenumbers

The instability studied here focuses on the physically acceptable case when both l and m have integer values. From a purely mathematical point the eigenvalue problem posed by Eq. (1) can also be solved for fractional wavenumber values. In cases when the algebraic radial structure describes the entire vortex (i.e., both in the inner region and the outer region, e.g., $\Psi(r) = (1 + r^b)^{-a}$, $r \geq 0$, so that the PV is continuous) such instabilities were indeed found by Gent and McWilliams (1986) and by Peng and Williams (1991). For these structures the conclusion of section 3 on the stability of algebraic radial decay does not hold since the mean PV does have an inflection point. (The explicit expression of Q_r is too cumbersome to analyze analytically but numerical calculations have demonstrated it.) Although the necessary condition for instability is satisfied, in many of these cross sections the instability is limited to fractional values of l, m only, for example, for $b = 2$ and $a = 0.5$, 1, 2 the $m = 0$ curves in Fig. 5 of Gent and McWilliams (1986) are limited to $1 < l < 1.6$ only. There are, however, other (a, b) values (and wavenumbers), especially when the algebraic decay at intermediate r is fast enough ($b = 4$), where the growth rate does not vanish at integer (l, m) values. The change in the instability characteristics of the present study, where the instability curve is continuous as a function of a, is attributed to the discontinuity of PV at $r = 1$.

We can summarize the results obtained in this study as follows.

1) The discontinuity in PV makes all SCVs observed in the ocean highly unstable with growth rates on the order of 1 day. The particular form assumed for cross section of angular velocity (and PV) in either the inner region or the outer one plays a very minor role in determining the growth rates as long as the PV cross section is discontinuous.

2) This instability is encountered even when the cross section does not satisfy the inflection point necessary condition for instability. When the PV distribution both satisfies the inflection point criterion and has a discontinuity, the latter dominates the growth rate. In this respect, a PV jump at the perimeter of the inner region has the same (or even stronger) destabilizing effect as compared with that of the inflection point in PV. A similar destabilizing effect of a discontinuity in PV was demonstrated by Boss et al. (1996) for two-layer fronts.

3) For all observed cross sections no instabilities were found for barotropic ($m = 0$) perturbations with azimuthal wavenumber 1.

Acknowledgments. I wish to acknowledge the hospitality extended to me while visiting GSO/URI. Support for this work was provided by the Israel Academy of Sciences through a research grant to The Hebrew University of Jerusalem. G. Flierl has provided important input and detected an error in an earlier version of this work. The programming assistance of Mrs. N. Porat and Mr. M. Frumin are gratefully appreciated. The comments of an anonymous reviewer improved the presentation of this work.

REFERENCES

Armi, L., and W. Zenk, 1984: Large lenses of highly saline Mediterranean water. *J. Phys. Oceanogr.*, **14,** 1560–1576.

Boss, E., N. Paldor, and L. Thompson, 1996: Stability of a potential vorticity front: from quasi-geostrophy to shallow water. *J. Fluid Mech.*, **315,** 65–84.

Chan, J. C., and R. T. Williams, 1987: Analytical and numerical studies of the β-effect in tropical cyclone motion. Part I: Zero mean flow. *J. Atmos. Sci.*, **44,** 1257–1265.

D'Asaro, E. A., 1988: Observations of small eddies in the Beaufort Sea. *J. Geophys. Res.*, **93** (C6), 6669–6684.

Drazin, P. G., and L. N. Howard, 1966: Hydrodynamic stability of parallel flow of inviscid fluid. *Adv. Appl. Mech.,* **9,** 1–89.

Elliott, B. A., and T. B. Sanford, 1986a: The subthermocline lens D1. Part I: Description of water properties and velocity profiles. *J. Phys. Oceanogr.,* **16,** 532–548.

——, and ——, 1986b: The subthermocline lens D1. Part II: Kinematics and dynamics. *J. Phys. Oceanogr.,* **16,** 549–561.

Fjortoft, R., 1950: Application of integral theorems in deriving criteria of stability for laminar flows and for the baroclinic circular vortex. *Geophys. Publ.,* **17** (6), 1–52.

Flierl, G. R., 1988: On the instability of geostrophic vortices. *J. Fluid Mech.,* **97,** 349–388.

Gent, P. R., and J. C. McWilliams, 1986: The instability of barotropic circular vortices. *Geophys. Astrophys. Fluid Dyn.*, **35,** 209–233.

Manley, T. O., and K. H. Hunkins, 1985: Mesoscale eddies of the Arctic Ocean. *J. Geophys. Res.*, **90** (C6), 4911–4930.

Newton, J. L., K. Aagaard, and L. K. Coachman, 1974: Baroclinic eddies in the Arctic Ocean. *Deep-Sea Res.*, **21,** 707–719.

Olson, D. B., 1991: Rings in the ocean. *Annu. Rev. Earth Sci.,* **19,** 283–311.

Paldor, N., and M. Ghil, 1990: Finite-wavelength instability of a coupled density front. *J. Phys. Oceanogr.,* **20,** 114–123.

—— and D. Nof, 1991: Linear instability of an anticyclonic vortex in a two-layer ocean. *J. Geophys. Res.*, **95** (C10), 18 075–18 079.

Peng, S. M., and R. T. Williams, 1990: Dynamics of vortex asymmetries and their influence on vortex motion on a β-plane. *J. Atmos. Sci.,* **47,** 1987–2003.

—— and ——, 1991: Stability analysis of barotropic vortices. *Geophys. Astrophys. Fluid Dyn.,* **58,** 263–283.

Prater, M. D., and T. B. Sanford, 1994: A meddy off Cape St. Vincent. Part I: Description. *J. Phys. Oceanogr.,* **24,** 1572–1586.

Riser, S. C., H. Freeland, and H. T. Rossby, 1978: Mesoscale motions near the deep western boundary of the North Atlantic. *Deep-Sea Res.,* **25,** 1179–1191.

——, W. B. Owens, H. T. Rossby, and C. C. Ebbesmeyer, 1986: The structure, dynamics and origin of a small-scale lens of water in the western North Atlantic thermocline. *J. Phys. Oceanogr.,* **16,** 572–590.

Schultz Tokos, K., and H. T. Rossby, 1991: Kinematics and dynamics of a Mediterranean salt lens. *J. Phys. Oceanogr.,* **21,** 879–892.

Walsh, D., 1995: A model of a mesoscale lens in large-scale shear. Part I: Linear calculations. *J. Phys. Oceanogr.,* **25,** 735–746.